Coupling light into few-mode optical fibres I: The diffraction limit

Anthony J. Horton and Joss Bland-Hawthorn

Anglo-Australian Observatory, PO Box 296, Epping, NSW, Australia

ajh@aao.gov.au

Abstract: Multimode fibres are widely used in astronomy because of the ease of coupling light into them at a telescope focus. The photonics industry has given rise to a broad range of products but these are almost exclusively restricted to single-mode fibres, although some can be adapted for use in fibres that allow several modes to propagate. Now that astronomical telescopes are moving toward diffraction-limited performance through the use of adaptive optics (AO), we address the problem of coupling light into a few-mode fibre (FMF). We find that fibres with as few as $\sim$5 guided modes share important characterisitcs with multimode fibres, in particular high coupling efficiency. We anticipate that future astronomical instruments at an AO-corrected focus will be able to exploit a broad class of photonic devices.

OCIS codes: (060.2310) Fibers optics; (010.1080) Adaptive optics; (060.2430) Fibers, single-mode; (999.9999) Fibers, few-mode

References and links

1. J. M. Hill, J. R. P. Angel, J. S. Scott, D. Lindley, and P. Hintzen, "Multiple object spectroscopy - The Medusa spectrograph," Astrophys. J. **242**, L69–L72 (1980).
2. M. Colless, G. Dalton, S. Maddox, W. Sutherland, P. Norberg, S. Cole, J. Bland-Hawthorn, T. Bridges, R. Cannon, C. Collins, W. Couch, N. Cross, K. Deeley, R. De Propris, S. P. Driver, G. Efstathiou, R. S. Ellis, C. S. Frenk, K. Glazebrook, C. Jackson, O. Lahav, I. Lewis, S. Lumsden, D. Madgwick, J. A. Peacock, B. A. Peterson, I. Price, M. Seaborne, and K. Taylor, "The 2dF Galaxy Redshift Survey: spectra and redshifts," MNRAS **328**, 1039–1063 (2001).
3. S. M. Croom, R. J. Smith, B. J. Boyle, T. Shanks, L. Miller, P. J. Outram, and N. S. Loaring, "The 2dF QSO Redshift Survey - XII. The spectroscopic catalogue and luminosity function," MNRAS **349**, 1397–1418 (2004).
4. D. G. York, J. Adelman, J. E. Anderson, S. F. Anderson, J. Annis, N. A. Bahcall, J. A. Bakken, R. Barkhouser, S. Bastian, E. Berman, W. N. Boroski, S. Bracker, C. Briegel, J. W. Briggs, J. Brinkmann, R. Brunner, S. Burles, L. Carey, M. A. Carr, F. J. Castander, B. Chen, P. L. Colestock, A. J. Connolly, J. H. Crocker, I. Csabai, P. C. Czarapata, J. E. Davis, M. Doi, T. Dombeck, D. Eisenstein, N. Ellman, B. R. Elms, M. L. Evans, X. Fan, G. R. Federwitz, L. Fiscelli, S. Friedman, J. A. Frieman, M. Fukugita, B. Gillespie, J. E. Gunn, V. K. Gurbani, E. de Haas, M. Haldeman, F. H. Harris, J. Hayes, T. M. Heckman, G. S. Hennessy, R. B. Hindsley, S. Holm, D. J. Holmgren, C.-h. Huang, C. Hull, D. Husby, S.-I. Ichikawa, T. Ichikawa, Ž. Ivezić, S. Kent, R. S. J. Kim, E. Kinney, M. Klaene, A. N. Kleinman, S. Kleinman, G. R. Knapp, J. Korienek, R. G. Kron, P. Z. Kunszt, D. Q. Lamb, B. Lee, R. F. Leger, S. Limmongkol, C. Lindenmeyer, D. C. Long, C. Loomis, J. Loveday, R. Lucinio, R. H. Lupton, B. MacKinnon, E. J. Mannery, P. M. Mantsch, B. Margon, P. McGehee, T. A. McKay, A. Meiksin, A. Merelli, D. G. Monet, J. A. Munn, V. K. Narayanan, T. Nash, E. Neilsen, R. Neswold, H. J. Newberg, R. C. Nichol, T. Nicinski, M. Nonino, N. Okada, S. Okamura, J. P. Ostriker, R. Owen, A. G. Pauls, J. Peoples, R. L. Peterson, D. Petravick, J. R. Pier, A. Pope, R. Pordes, A. Prosapio, R. Rechenmacher, T. R. Quinn, G. T. Richards, M. W. Richmond, C. H. Rivetta, C. M. Rockosi, K. Ruthmansdorfer, D. Sandford, D. J. Schlegel, D. P. Schneider, M. Sekiguchi, G. Sergey, K. Shimasaku, W. A. Siegmund, S. Smee, J. A. Smith, S. Snedden, R. Stone, C. Stoughton, M. A. Strauss, C. Stubbs, M. SubbaRao, A. S. Szalay, I. Szapudi, G. P. Szokoly, A. R. Thakar, C. Tremonti, D. L. Tucker, A. Uomoto, D. Vanden Berk, M. S. Vogeley, P. Waddell, S.-I. Wang, M. Watanabe, D. H. Weinberg, B. Yanny, and N. Yasuda, "The Sloan Digital Sky Survey: Technical Summary," AJ **120**, 1579–1587 (2000).

#76288 - $15.00 USD Received 20 October 2006; accepted 29 January 2007

5. J. Guerin and P. Felenbok, "Optical fibres for astronomical applications," in *Fiber Optics in Astronomy*, S. C. Barden, ed., vol. 3 of *ASP Conf. Ser.*, pp. 52–62 (1988).
6. C. Vanderriest, "Integral Field spectrography with Optical Fibres at C.F.H." in *Fiber Optics in Astronomy II*, P. M. Gray, ed., vol. 37 of *ASP Conf. Ser.*, pp. 338–+ (1993).
7. S. C. Barden and R. A. Wade, "DensePak and spectral imaging with fiber optics," in *Fiber Optics in Astronomy*, S. C. Barden, ed., vol. 3 of *ASP Conf. Ser.*, pp. 113–124 (1988).
8. J. Allington-Smith, G. Murray, R. Content, G. Dodsworth, R. Davies, B. W. Miller, J. Turner, I. Jorgensen, I. Hook, D. Crampton, and R. Murowinski, "The GMOS Integral Field Unit: First Integral Field Spectroscopy with an 8m Telescope (Invited Talk)," in *Galaxies: the Third Dimension*, M. Rosada, L. Binette, and L. Arias, eds., vol. 282 of *ASP Conf. Ser.*, pp. 415–+ (2002).
9. O. Le Fevre, M. Saisse, D. Mancini, G. P. Vettolani, D. Maccagni, J. P. Picat, Y. Mellier, A. Mazure, J. G. Cuby, B. Delabre, B. Garilli, L. Hill, E. Prieto, C. Voet, L. Arnold, S. Brau-Nogue, E. Cascone, P. Conconi, G. Finger, G. Huster, A. Laloge, C. Lucuix, E. Mattaini, P. Schipani, G. Waultier, F. M. Zerbi, G. Avila, J. W. Beletic, S. D'Odorico, A. F. Moorwood, G. J. Monnet, and J. Reyes Moreno, "VIMOS and NIRMOS multi-object spectrographs for the ESO VLT," in *Optical and IR Telescope Instrumentation and Detectors*, M. Iye and A. F. Moorwood, eds., vol. 4008 of *Proc. SPIE* , pp. 546–557 (2000).
10. J. Schmoll, G. N. Dodsworth, R. Content, and J. R. Allington-Smith, "Design and construction of the IMACS-IFU: a 2000-element integral field unit," in *Ground-based Instrumentation for Astronomy*, A. F. M. Moorwood and M. Iye, eds., vol. 5492 of *Proc. SPIE* , pp. 624–633 (2004).
11. I. Parry, A. Bunker, A. Dean, M. Doherty, A. Horton, D. King, M. Lemoine-Busserole, C. D. Mackay, R. McMahon, S. Medlen, R. G. Sharp, and J. Smith, "CIRPASS: description, performance, and astronomical results," in *Ground-based Instrumentation for Astronomy*, A. F. M. Moorwood and M. Iye, eds., vol. 5492 of *Proc. SPIE* , pp. 1135–1144 (2004).
12. S. Shaklan and F. Roddier, "Coupling starlight into single-mode fibre optics," Appl. Opt. **27**(11), 2334–2338 (1988).
13. J. Bland-Hawthorn and A. Horton, "Instruments without optics: an integrated photonic spectrograph," in *Ground-based and Airborne Instrumentation for Astronomy*, I. S. McLean and M. Iye, eds., vol. 6269 of *Proc. SPIE* (2006).
14. J. Bland-Hawthorn, M. Englund, and G. Edvell, "New approach to atmospheric OH suppression using an aperiodic fibre Bragg grating," Opt. Express **12**, 5902–5909 (2004).
15. V. Coudé du Foresto, M. Faucherre, N. Hubin, and P. Gitton, "Using single-mode fibers to monitor fast Strehl ratio fluctuations. Application to a 3.6 m telescope corrected by adaptive optics," A&AS **145**, 305–310 (2000).
16. S. G. Leon-Saval, T. A. Birks, J. Bland-Hawthorn, and M. Englund, "Multimode fiber devices with single-mode performance," Opt. Lett. **30**, 2545–2547 (2005).
17. D. Gloge, "Weakly Guiding Fibres," Appl. Opt. **10**(10), 2252–2258 (1971).
18. J. E. Midwinter, *Optical Fibres for Transmission* (Wiley, New York, 1979).
19. L. B. Jeunhomme, *Single-Mode Fibre Optics* (Marcel Dekker, New York, 1983).
20. D. Marcuse, *Theory of dielectric optical waveguides* (Academic Press, New York, 1974).

1. Introduction

Optical fibres have been in use in astronomical instrumentation for almost 30 years. They were first used for fibre-fed multi-object spectroscopy[1], where the efficiency gains from the ability to observe large numbers of objects at once have made many otherwise impractical scientific programmes possible [2, 3, 4]. Another important application is integral field spectroscopy[5, 6, 7], which is now a well established technique employed by a number of major optical and near infrared instruments [8, 9, 10, 11]. Optical fibres are also in use in astronomical optical interferometers [12].

The majority of fibre-fed instruments so far have been designed for operation under natural seeing conditions where the incoming light is aberrated by atmospheric effects, and the relative ease of coupling light into multimode fibres (MMFs) under these conditions has led to their exclusive use in instruments to date. Developments in astrophotonics now provide a strong motivation to move away from MMFs, however. Astrophotonics is a broad term used for the astronomical application of a wide range of photonic technology, and this burgeoning field has the potential to revolutionise astronomy. Important examples which are likely to have a significant impact in the near future are integrated photonic spectrographs[13] and OH suppression fibres based on aperiodic fibre Bragg gratings (AFBGs)[14]. These new devices are capable of

#76288 - $15.00 USD Received 20 October 2006; accepted 29 January 2007

greatly benefitting astronomy, however a significant obstacle to realising this potential is the fact that many have been conceived as single-mode devices, meaning that they cannot be fed by conventional MMFs.

The most obvious way to integrate such photonic devices into an instrument is to feed them with single-mode fibres (SMFs), but this approach has its own difficulties. Shaklan & Roddier[12] and Coudé du Foresto et al[15] have shown that the theoretical maximum efficiency with which a stellar image can be coupled into a single mode fibre is $\sim 80\%$ in the absence of any atmospheric turbulence effects or obstructions in the telescope pupil. When the effect of a reasonable circular central obstruction of 20% of the primary diameter is included this falls to $\sim 70\%$, and the presence of atmospheric aberrations further reduces the coupling efficiency approximately in proportion to the Strehl ratio. As a result direct coupling of large telescopes to SMFs in natural seeing, where the Strehl ratio is typically $< 1\%$, is rendered impractical by low efficiency. The use of adaptive optics (AO) to correct for atmospheric aberrations is widespread in modern astronomy, however the correction is not perfect and the use of SMFs places strong constraints on the necessary performance of the AO system, both in terms of the average Strehl achieved and its variability (which impacts on calibration).

While the continuing development of AO may allow highly efficient and stable coupling of telescopes to SMFs in the future there is an intermediate approach which should allow the efficient integration of astrophotonic devices now. Though many important devices are single-mode it is in general possible to extend them to operate with a few propagating modes. With OH suppressing fibres, for example, the atmospheric emission lines must be blocked separately for each propagating mode, which can be achieved either with a single, more complex AFBG or by using converters to connect to multiple single-mode AFBGs[16]. An integrated spectrograph can also be made to work with a few modes[13], at least at low and moderate resolutions. Using modified astrophotonic devices such as these makes it is possible to use few-mode fibres (FMFs) instead of SMFs. The coupling of light into FMFs is relatively unexplored territory, however as the number of modes increases it will become easier to couple light into the fibres, which is expected to reduce the sensitivity to AO system performance at the expense of increasing the required complexity of attached astrophotonic devices. In this paper we describe an ongoing investigation into the trade off between coupling efficiency and the number of propagating modes.

2. Theory

2.1. Fibre modes

We consider a conventional silica step-index fibre, consisting of a core of radius a with uniform refractive index n_1 surrounding by cladding material of uniform index $n_2 < n_1$, and follow the treatments of Gloge[17], Midwinter[18] and Jeunhomme[19]. In the limit of $\Delta = (n_1 - n_2)/n_2 \ll 1$ the propagating modes of such a fibre have a particularly simple form. In this 'weakly-guiding' limit the Maxwell equations can be transformed into a scalar wave equation for the longitudinal components, and the fields within the fibre expressed as a series of linearly polarised (LP) modes. In practice this is a reasonable approximation for a real fibre, as the difference in refractive indices is generally $< 1\%$ and the resulting error in mode characteristics $< 0.1\%$.

The LP modes are characterised by two numbers, the azimuthal order, l, and the radial order, m. The transverse component of the electric field of the LP_{lm} mode is given by

$$E_{lm}(\rho,\theta) = \quad A_{lm}(\sin l\theta, \cos l\theta) J_l(u_{lm}\rho)/J_l(u_{lm}) \quad \rho \leq 1 \tag{1}$$

$$A_{lm}(\sin l\theta, \cos l\theta) K_l(w_{lm}\rho)/K_l(w_{lm}) \quad \rho > 1, \tag{2}$$

where ρ is the normalised radial coordinate r/a, J_l is the Bessel function of the first kind of

#76288 - $15.00 USD Received 20 October 2006; accepted 29 January 2007

order l and K_l is corresponding modified Bessel function of the second kind. For each LP mode with $l \neq 0$ two independent orientations exist, with $\sin l\theta$ and $\cos l\theta$ azimuthal dependences. The longitudinal components are small compared to the transverse (by a factor $> 1/\sqrt{2\Delta}$) and can for most purposes be neglected.

The transverse propagation constants for the core (u_{lm}) and cladding (w_{lm}) are determined by the normalised frequency, V, which is defined by $V = 2\pi a \mathrm{NA}/\lambda$ where λ is wavelength and $\mathrm{NA} = (\mathrm{n}_1^2 - \mathrm{n}_2^2)^{1/2} \approx \mathrm{n}_2\sqrt{2\Delta}$ is the numerical aperture of the fibre. The transverse propagation constants satisfy

$$V = (u^2 + w^2)^{1/2} \tag{3}$$

and u_{lm},w_{lm} are given by the mth root of

$$u\frac{J_{l-1}(u)}{J_l(u)} + w\frac{K_{l-1}(w)}{K_l(w)} = 0. \tag{4}$$

From Eqs. (3) and (4) it can be shown that u_{lm} must lie between the mth zero of J_{l-1} and the mth zero of J_l. For a mode to be guided by the fibre w_{lm} must be real, and so the minimum value of u_{lm} defines the cutoff frequency, V_c, for the mode. In the special case of $l = 0$ the $m = 1$ mode has a cutoff frequency of zero, this is the fundamental mode of the fibre and is always present. For a more rigorous treatment of the cutoff conditions see, for example, Marcuse[20]. The cutoff frequencies of the first few LP modes are given in Table 1. As can be seen from the table the cutoff frequencies of the LP modes become more closely spaced at higher frequencies, in fact the number of guided modes at a normalised frequency V is approximately proportional to V^2.

Table 1. Cutoff frequencies for the linearly polarised modes of a step index fibre.

l	m	V_c	l	m	V_c	l	m	V_c	l	m	V_c
0	1	0.000	4	1	6.380	6	1	8.771	5	2	11.065
1	1	2.405	0	3	7.016	4	2	9.761	8	1	11.619
0	2	3.832	2	2	7.016	7	1	9.936	1	4	11.792
2	1	3.832	5	1	7.588	0	4	10.173	9	1	12.225
3	1	5.136	3	2	8.417	2	3	10.173	6	2	12.339
1	2	5.520	1	3	8.654	3	3	11.086	4	3	13.015

2.2. Image field

The field distribution in the focal plane of a telescope is related to the distribution in the entrance pupil by

$$\mathbf{E}_{\mathrm{focus}}(\mathbf{r}) \propto \tilde{\mathbf{E}}_{\mathrm{pupil}}\left(\frac{\mathbf{r}}{\lambda f}\right) \tag{5}$$

where the tilde represents a Fourier transform and f is the effective focal length of the telescope. The field in the entrance pupil can be written as

$$\mathbf{E}_{\mathrm{pupil}}(\mathbf{r}') = \mathbf{E}_\star P(\mathbf{r}')\Psi(\mathbf{r}') \tag{6}$$

where $E_\star$ is the field received from the source, P is the pupil transmission function and Ψ is a phase screen which incorporates any optical aberrations, either fixed aberrations inherent to the

#76288 - $15.00 USD Received 20 October 2006; accepted 29 January 2007

telescope optics or random, variable aberrations due to passage of the incoming light through turbulence in the atmosphere.

Initially we consider the diffraction limited case where there are no aberrations, i.e. $\Psi = 1$. If we represent the telescope pupil as a circular aperture of radius R with a central obstruction of radius αR then the focal plane field distribution for a point source is given by

$$\mathbf{E}_{\text{focus}} = \mathbf{E}_0 \left[\frac{2J_1(s)}{s} - \alpha^2 \frac{2J_1(\alpha s)}{\alpha s}, \right] \tag{7}$$

where s is a scaled radial coordinate given by $s = 2\pi Rr/\lambda f$. Noting that $2R/f$ is the definition of focal ratio of the telescope, F, we see that the dimensions of the diffraction limited image scale in proportion to the product λF.

2.3. Coupling efficiency

The fraction of incident energy which is coupled into an individual mode, ε_{lm}, can be calculated from the electric field distribution of the image $\mathbf{E}_{\text{focus}}$ and that of the fibre mode $\mathbf{E}_{lm}$ according to

$$\varepsilon_{lm} = \frac{\left| \int_\infty \mathbf{E}^*_{\text{focus}} \cdot \mathbf{E}_{lm} \mathrm{d}A \right|^2}{\int_\infty |\mathbf{E}_{\text{focus}}|^2 \mathrm{d}A \int_\infty |\mathbf{E}_{lm}|^2 \mathrm{d}A}. \tag{8}$$

The asterisk indicates complex conjugation and the integrals are performed over an infinite plane at the telescope focus. When ignoring polarisation and by noting that the electric field of the incident light is purely transverse we can rewrite Eq. (8) in terms of inner products of the transverse field component distributions, i.e.

$$\varepsilon_{lm} = \frac{|\langle E_{\text{focus}} | E_{lm} \rangle|^2}{\langle E_{\text{focus}} | E_{\text{focus}} \rangle \langle E_{lm} | E_{lm} \rangle} \tag{9}$$

where E_{focus} is the scalar part of Eq. 7 and E_{lm} is the transverse component of the LP_{lm} mode field as in Eqs. (1) and (2). In writing Eq. (9) we have also used the fact that the longitudinal field components of an LP mode are small relative to the transverse components (see Sect. 2.1) to neglect their contribution to $\int_\infty |\mathbf{E}_{lm}|^2 \mathrm{d}A$.

The coupling efficiency ε, defined as the fraction of the incident energy which ends up being guided by the fibre, is simply given by summing the ε_{lm} over all the guided modes.

3. Initial results

3.1. Model system

In the calculations described here we use diffraction limited images coupled directly into a step index fibre in the focal plane. Such a system can be characterised by three dimensionless parameters, S, α and V. The parameter $S = \lambda F/a$ determines the scale of the image relative to the fibre core, the central obstruction size α determines the form of the image, and the normalised frequency $V = 2\pi a \text{NA}/\lambda$ determines the number and form of the guided modes. However instead of presenting our results in terms of these generalised parameters we prefer to work with the more physical set of variables F, α and $d = 2a$, and assume appropriate values for λ and NA. The results can of course be transformed to other wavelengths or NAs via the corresponding values of S and V.

The wavelengths and NA used have been chosen to be representative of likely values for an astrophotonics application. The astronomical H-band wavelength region (~ 1.45–1.75μm) is of particular interest as this is the region being targeted by the first generation of OH suppression AFBGs, and FMF coupling will play an important role in integrating these devices into full

#76288 - $15.00 USD Received 20 October 2006; accepted 29 January 2007

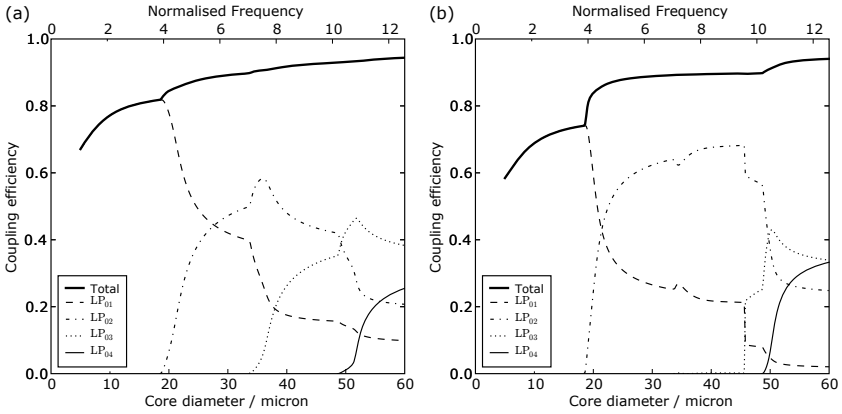

Fig. 1. Maximum coupling efficiency versus core diameter for an NA $= 0.1$ fibre at a wavelength of 1.5μm. The overall coupling efficiency and the contributions from each fibre mode are shown for (a) $\alpha = 0$ and (b) $\alpha = 0.2$.

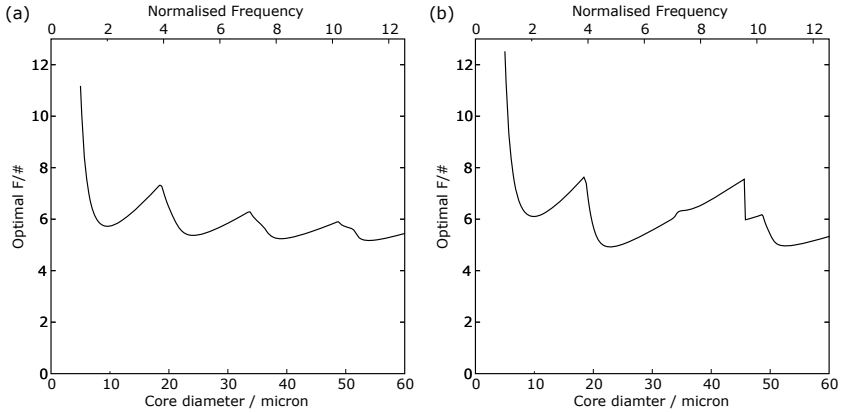

Fig. 2. Optimal focal ratio versus core diameter for an NA $= 0.1$ fibre at a wavelength of 1.5μm. The focal ratio corresponding to maximum coupling efficiency is shown for (a) $\alpha = 0$ and (b) $\alpha = 0.2$.

scale astronomical instruments. For this reason we have used H-band wavelengths in these calculations, selecting 1.5μm as representative. Ordinary silica optical fibres typically have numerical apertures in the range 0.1–0.2, with SMFs generally towards the lower end of this range and MMFs higher. For these calculations we have used an NA of 0.1.

3.2. Maximum coupling efficiency versus core diameter

The first result from these investigations was the dependence of maximum coupling efficiency on the fibre core diameter. To calculate this the coupling efficiency was optimised against focal ratio for core diameters in the range 5–60μm. For $\lambda = 1.5\mu$m and NA $= 0.1$ this range of core diameters corresponds to a range in normalised frequency of 1.05–12.6, which as can be seen from Table 1 covers single mode operation at the lower end ($d < 11.5\mu$m) up to 23 guided

#76288 - $15.00 USD Received 20 October 2006; accepted 29 January 2007

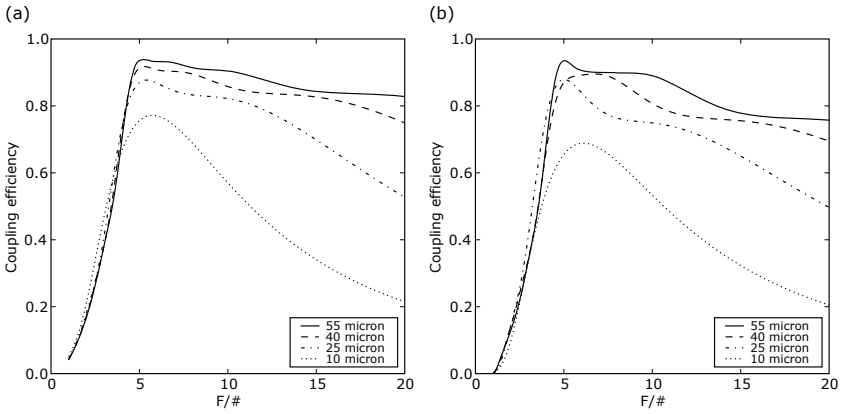

Fig. 3. Coupling efficiency versus focal ratio for an NA $= 0.1$ fibre at a wavelength of 1.5μm. Coupling efficiency is shown for core diameters of 10, 25, 40 and 55μm with (a) $\alpha = 0$ and (b) $\alpha = 0.2$.

modes at the upper limit.

The results are shown in Fig. 1(a) and Fig. 1(b) for $\alpha = 0$ and $\alpha = 0.2$ respectively. The two values of α represent the ideal case and one more typical of the current generation of large telescopes. In both cases there is a monotonic increase in total coupling efficiency as the core diameter increases (from 67% to 94% for $\alpha = 0$, 58% to 94% for $\alpha = 0.2$) punctuated by a number of discontinuities in the gradient. From these results we immediately see that FMFs give significantly higher maximum coupling efficiency than SMFs ($d < 11.5\mu$m), especially in the more realistic $\alpha = 0.2$ case. The cause of the discontinuities becomes apparent when the contributions from each of the guided modes are examined so these have also been plotted on Fig. 1. In this calculation the image is aligned with the fibre axis and due to the axial symmetry only $l = 0$ modes contribute. In the $\alpha = 0$ case the position of the discontinuities coincides with the cutoff frequencies of the LP_{02}, LP_{03} and LP_{04} modes, and it is the appearance of these modes that provides a boost to the coupling efficiency. The $\alpha = 0.2$ case is slightly more complex as the different image profile results in significant jumps in coupling efficiency at the appearance of the LP_{02} and LP_{04} modes while the LP_{03} mode does not contribute until well above its cutoff.

The significant negative effect on SMF coupling efficiency of a central obstruction in the telescope pupil was previously noted by Coude du Foresto et al[15], and a comparison of the small core diameter ends of Fig. 1(a) and Fig. 1(b) shows that an efficiency loss of $\sim 10\%$ occurs with $\alpha = 0.2$. The effect of the central obstruction on the image is to reduce the field strength in the central peak while increasing it in the first ring, which reduces the coupling to the LP_{01} mode. This change in image profile increases the coupling to the LP_{02} mode, however, and so above the LP_{02} cutoff we see the maximum coupling efficiency for $\alpha = 0.2$ approximately equal that for $\alpha = 0$. Similarly the $\alpha = 0.2$ image does not couple well to the LP_{03} mode, but does to LP_{04}.

3.3. Focal ratio dependence

In calculating the maximum coupling efficiency as a function of core diameter we also obtained the focal ratios at which maximum coupling efficiency is achieved. These optimal focal ratios are shown in Figs. 2(a) and 2(b) for the $\alpha = 0$ and $\alpha = 0.2$ cases. To get a fuller picture of the

#76288 - $15.00 USD Received 20 October 2006; accepted 29 January 2007

effect of focal ratio we also calculated coupling efficiency for $F = 1$–20 for four core diameters of 10, 25, 40, 55μm. With NA $= 0.1$ and $\lambda = 1.5\mu$m these core diameters have one, two, three and four guided $l = 0$ modes respectively. The results for $\alpha = 0$ and $\alpha = 0.2$ are plotted as Fig. 3(a) and Fig. 3(b).

The mode cutoffs and changes in the contributions of each mode seen in Fig. 1 are also seen reflected in variations in the optimal focal ratio in Fig. 2, however as the diameter increases the variations diminish and the optimal focal ratio converges from above on a value of ~ 5. In other words the optimal image size does not scale with the fibre diameter but instead remains relatively constant. Looking at Fig. 3 we see that for all the plotted core diameters the coupling efficiency declines rapidly for focal ratios less than ~ 5. This low F cutoff is the same as predicted in the multi-mode limit via geometric optics. By considering the condition for total internal reflection to occur at the core/cladding interface the numerical aperture of the fibre can be equated to the sine of the maximum angle of incidence at which a light ray can strike the fibre face and still be guided within the core. This maximum angle can then be converted into a minimum focal ratio via $F_{\mathrm{min}} = \frac{1}{2}\tan\left(\sin^{-1}\mathrm{NA}\right) \approx 1/(2.\mathrm{NA})$, and for an NA of 0.1 this is 4.97. So we see that the geometric optics derived maximum focal ratio for MMFs also applies to the single and few-mode regime, and furthermore the optimum focal ratio for FMFs lies close to this value.

The other main feature of Fig. 3 is the decreasing sensitivity of the coupling efficiency to higher than optimum focal ratios as the core diameter increases. This would be intuitively expected as the larger core allows for greater magnification of the image (higher F) before a significant proportion of the light falls outside the core. Upon examining the contributions of the individual modes as the focal ratio changes it is also possible to explain a number of the features in the coupling efficiency slope, which are particularly apparent in the $\alpha = 0.2$ case. As the focal ratio increases the lower order modes become progressively more important and so, for instance, the significant decline in coupling efficiency between $F = 5$ and $F = 7$ for a 25μm core when $\alpha = 0.2$ is due to a decline in the LP_{02} mode and a transition to dominance by the poorly coupling LP_{01} mode. The other features can be similarly ascribed to the decline of particular modes.

3.4. Sensitivity to decentring

While the increases seen in maximum coupling efficiency with only a few additional modes are pleasing, the primary motivation for undertaking this investigation is the expectation that FMF coupling efficiency will be considerably less sensitive than SMFs to deviations from ideal conditions, thereby making them a more practical option for real world applications. In order to determine to what extent this is true we must calculate the effect of realistic aberrations on the coupling efficiency. However, at the time of writing, the only aspect of this analysis which is complete is an examination of the effect of displacing the image centre from the fibre axis. Such displacements are certain to occur to some degree in astronomical use for a number of reasons such as imperfect correction of wavefront tip/tilt, finite fibre positioner precision and finite accuracy of astrometry.

Figure 4 shows the coupling efficiency as a function of image decentring for 10, 25, 40 and 55μm diameter cores. For these calculations there is no axial symmetry and so all the guided modes must be included, not just the $l = 0$ ones. With NA $= 0.1$ and $\lambda = 1.5\mu$m the four core diameters give 1, 5, 10 and 19 guided modes respectively. The previously calculated focal ratios for maximum (on-axis) coupling efficiency were used for each diameter. For simplicity only the $\alpha = 0$ case is shown, but the $\alpha = 0.2$ results are similar. There is a qualitative difference in behaviour here between SMFs and FMFs, whereas fibres with 5 or more modes show variations in coupling efficiency of only $\sim 5\%$ for decentres up to 80% of the core radius the single-mode

#76288 - $15.00 USD Received 20 October 2006; accepted 29 January 2007

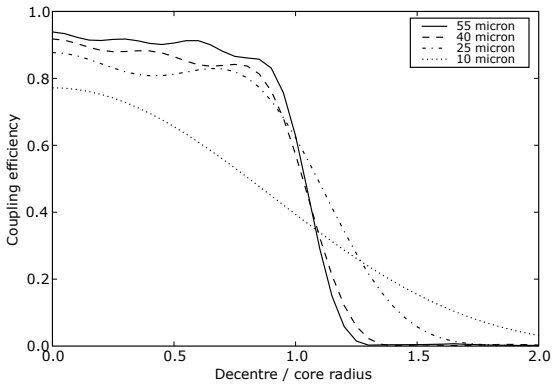

Fig. 4. Coupling efficiency versus decentring of the image centre from the fibre axis. Coupling efficiency is shown for NA $= 0.1$ fibres with 10, 25, 40 and 55μm core diameters at a wavelength of 1.5μm and with $\alpha = 0$.

fibre loses over a third of its coupling efficiency over the same range. This flat response is a desirable property of the FMFs as it means that moderate image-fibre misalignments will not cause drops in throughput and attendant calibration issues.

Knowing the dependence of point source coupling efficiency on image position also enables us to calculate the coupling efficiency for an extended source. For an extended source with an angular intensity distribution on the sky of $I_{\rm ext}(\theta)$ the effective coupling efficiency $\varepsilon_{\rm ext}$ is given by

$$\varepsilon_{\rm ext} = \frac{\int_\infty \varepsilon_{\rm psf}(\mathbf{r}) I_{\rm ext}(\mathbf{r}/f)\mathrm{dA}}{\int_\infty I_{\rm ext}(\mathbf{r}/f)\mathrm{dA}} \tag{10}$$

where $\varepsilon_{\rm psf}(\mathbf{r})$ is the coupling efficiency for a point source image centred on a position $\mathbf{r}$ in the focal plane. This is in effect taking a weighted average of the coupling efficiency over the area of the source image, and so while the exact figure will depend on the shape and size of the source what can be said is that the flatter responses seen with the FMFs will further increase their coupling efficiency advantage over SMFs for resolved sources.

We can also calculate the effective solid angle of sky coupled into the fibre, $\Omega_{\rm sky} = \pi(a/f)^2 \int_\infty \varepsilon_{\rm psf}\mathrm{dA}$. For the core diameters considered here we find $\int_\infty \varepsilon_{\rm psf}\mathrm{dA} \approx 1$ (0.98, 1.10, 0.93 and 0.96) and so $\Omega_{\rm sky} \approx \pi D^2 (a/F)^2$, the same result as would be derived from geometric optics. This strong dependence of the sky background on $(a/F)^2$ together with the previously established relative insensitivity of FMF coupling efficiency to increasing F (see Fig. 3) means that the focal ratio which maximises signal-to-noise ratio will in general be larger than the optimal value for coupling efficiency, and except for very bright sources will be that which matches the scale of the source image to the core size, the same as for the MMFs.

3.5. Wavelength dependence

The previous calculations have been performed for a single wavelength, however astronomical applications generally require good performance over a wide wavelength range. Figure 5 shows coupling efficiency as a function of wavelength for NA $= 0.1$ fibres with core diameters of 10, 25, 40 and 55μm. For each diameter the focal ratio was fixed at the optimal value for 1.6μm while the wavelength was varied over the range 1.4–1.8μm. This wavelength range encompasses the whole of the $\sim$1.45–1.75μm H-band, which is of particular interest due to

#76288 - $15.00 USD Received 20 October 2006; accepted 29 January 2007

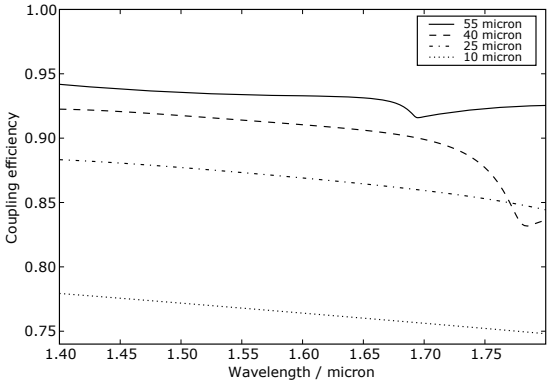

Fig. 5. Coupling efficiency versus wavelength for NA $= 0.1$ fibres with core diameters of 10, 25, 40 and 55μm, and with $\alpha = 0$. For each diameter the focal ratio was fixed at the optimal value for a wavelength of 1.6μm.

its connection with OH suppression fibre developments. Only $\alpha = 0$ results are shown, but $\alpha = 0.2$ is similar. The general trend for all core diameters is a gradual decrease in coupling efficiency of $\sim 3\%$ over the wavelength range, however for the 40 and 55μm core diameters there is a significant dip superimposed on this steady decline. For the 40μm core this feature corresponds to the LP_{03} mode cutoff, while for 55μm the LP_{04} mode cutoff is the cause. So we see that in general SMFs and FMFs exhibit good broadband performance, however it would be best to chose fibre parameters so as to avoid an $l = 0$ mode cutoff falling within an operational wavelength band.

4. Discussion

Astrophotonic developments such as OH suppression fibres and integrated photonic spectrographs have enormous potential, however efficiently integrating them into an astronomical instrument presents a challenge. The MMFs conventionally used in astronomy, while efficient at accepting starlight, are not suitable for feeding light into these devices as the devices are not able to accept a large number of modes. SMFs, on the other hand, while ideal for feeding light into astrophotonic devices are difficult to couple starlight into, even with adaptive optics. We have begun an investigation into the intermediate territory of FMFs, in order to find the best compromise between the two extremes.

Our initial results on diffraction limited fibre coupling have shown that FMFs exhibit many of the desirable properties of MMFs even when there are only of order 10 guided modes. For example, FMFs offer higher maximum coupling efficiency than SMFs ($> 90\%$), especially for extended sources. Also FMFs are less sensitive to the effects of obstructions in the telescope pupil than SMFs are. Unlike SMFs, FMFs can efficiently couple light over a range of focal ratios from $F_{\min} \approx 1/(2.\mathrm{NA})$ up to a maximum value determined by matching the size of the image to the fibre core. FMFs are also tolerant of displacement of the image centre from the fibre axis, provided the image remains within the fibre core. Both SMFs and FMFs exhibit little sensitivity to wavelength.

While these results are encouraging the use of perfect diffraction limited images does represent an idealised case. In any real ground based telescope the adaptive optics correction will be imperfect, and the residual atmospheric wavefront perturbations will effect the coupling ef-

#76288 - $15.00 USD Received 20 October 2006; accepted 29 January 2007

ficiency. It is known that SMF coupling is highly sensitive to imperfect correction, with the coupling efficiency declining in proportion to the Strehl ratio[15], however the corresponding dependency for FMFs has not previously been investigated. Ongoing work, to be presented in a second paper, aims to determine the dependence of FMF coupling efficiency on the order of correction, from the diffraction limit to natural seeing, and thereby establish the number of modes required for acceptable throughput levels under a range of realistic usage conditions.

Preliminary results have also been obtained for pupil-plane coupling to FMFs, which show a similar rapid convergence on MMF behaviour above ~ 10 modes as the image-plane results discussed here. This work will be extended to model lenslet arrays of various geometries and both image and pupil-plane coupling with a view to determining the best approach for FMF integral field spectroscopy.

Acknowledgments

The authors gratefully acknowledge the support of PPARC research grant PP/D002494/1 for this programme of work.

#76288 - $15.00 USD Received 20 October 2006; accepted 29 January 2007